Article

CeO$_2$ Nanomaterials from Diesel Engine Exhaust Induce DNA Damage and Oxidative Stress in Human and Rat Sperm In Vitro

Martina Cotena [1,2], Mélanie Auffan [2,3], Stéphane Robert [4], Virginie Tassistro [1], Noémie Resseguier [5], Jérôme Rose [2,3] and Jeanne Perrin [1,6,*]

[1] IMBE, CNRS, IRD, Avignon Université, Aix Marseille University, 13005 Marseille, France; martina.cotena@univ-amu.fr (M.C.); virginie.tassistro@univ-amu.fr (V.T.)

[2] CEREGE, Europole Arbois, BP 80, CNRS, IRD, INRAE, Coll France, Aix Marseille University, 13545 Aix en Provence, France; auffan@cerege.fr (M.A.); rose@cerege.fr (J.R.)

[3] Civil and Environmental Engineering, Duke University, Durham, NC 27708, USA

[4] AMUTICYT Core Facility, UMR1263, INSERM, INRAE, Aix Marseille University, 13005 Marseille, France; stephane.robert@univ-amu.fr

[5] Department of Biostatistics and Public Health, La Timone Hospital, 13005 Marseille, France; noemie.resseguier@univ-amu.fr

[6] Laboratory of Reproduction Biology-CECOS, Department of Gynecology, Obstetrics and Reproductive Medicine, AP-HM La Conception, Pôle Femmes Parents Enfants, 13005 Marseille, France

* Correspondence: jeanne.perrin@univ-amu.fr

check for updates

Abstract: Cerium dioxide nanomaterials (CeO$_2$ NMs) are widely used in nano-based diesel additives to decrease the emission of toxic compounds, but they have been shown to increase the emission of ultrafine particles as well as the amount of released Ce. The Organization for Economic Cooperation and Development included CeO$_2$ NMs in the priority list of nanomaterials that require urgent evaluation, and the potential hazard of aged CeO$_2$ NM exposure remains unexplored. Herein, human and rat sperm cells were exposed in vitro to a CeO$_2$ NM-based diesel additive (called Envirox^{TM}), burned at 850 °C to mimic its release after combustion in a diesel engine. We demonstrated significant DNA damage after in vitro exposure to the lowest tested concentration (1 μg·L^{-1}) using the alkaline comet assay (ACA). We also showed a significant increase in oxidative stress in human sperm after in vitro exposure to 1 μg·L^{-1} aged CeO$_2$ NMs evaluated by the H$_2$DCF-DA probe. Electron microscopy showed no internalization of aged CeO$_2$ NMs in human sperm but an affinity for the head plasma membrane. The results obtained in this study provide some insight on the complex cellular mechanisms by which aged CeO$_2$ NMs could exert in vitro biological effects on human spermatozoa and generate ROS.

Keywords: nanoparticles; DNA damage; Oxidative stress; reproductive toxicity; combustion; ageing; NMs life cycle

1. Introduction

Nanoparticles (NPs) and nanomaterials (NMs), particularly metal oxide NMs, are increasingly used in many fields of everyday life, e.g., food packaging, cosmetics, textiles, electronics, and even biomedicine. Extensive usage of NMs in various areas has raised human health concerns, mostly in terms of occupational exposure [1,2]. Considering the life cycle of nano-enabled products (from the production and formulation stage to their usage and end of life), the occupational exposure of workers to NMs [3] has been more studied than others viz., consumer and environmental exposures. The reason

is the presence of non-nano-specific regulations, which put worker protection at the forefront with efficient individual protection equipment [4]. Consequently, major knowledge gaps remain in the risk assessment of NMs, especially in the post-production stages of their life cycle [5], e.g., people/consumers are directly or indirectly exposed during use or during waste treatment.

Among all, CeO_2 NMs have been increasingly used in Europe and elsewhere as fuel-borne catalysts in diesel engines [6,7] as the Envirox^{TM} from Energenics Europe Ltd. The addition of CeO_2 NMs in diesel has been reported to increase the fuel combustion efficiency [8] and decrease the emission of CO_2, CO, the total particulate mass, formaldehyde, acetaldehyde, acrolein, and several polycyclic aromatic hydrocarbons [9] during combustion. However, it has also been shown to increase the emission of ultrafine particles, NOx, and benzo[a]pyrene as well as the amount of Ce released in natural environments (air, water, soil) near roads [10,11]. In the UK, near an urban road where Envirox^{TM} is known to be used, an increase in ambient Ce-based NMs was observed with a concentration of $\sim$0.3 ng$\cdot$m^{-3} and aerodynamic diameters peaking at 150 nm [12]. To date, there are large uncertainties regarding the acceptable level of Ce-based NMs in the atmosphere because most toxicity studies have been done with pristine CeO_2 NMs that are not representative of the emission in diesel exhaust. Indeed, once released in the atmosphere after combustion in a diesel engine, Ce is in the form of CeO_2 NMs with different physical-chemical properties compared to pristine CeO_2 NMs (in terms of size, surface properties, mineralogy, aggregation state, solubility) [4], which can affect their fate, bioavailability [13,14] and potential toxicity [2,15]. Therefore, investigating the potential adverse effects of such combusted CeO_2 NMs on human health represents an important step in the safety assessment required from Registration, Evaluation, Authorisation and Restriction of Chemicals (REACH) and from the Organization for Economic Cooperation and Development (OECD's guidelines 2011) [16,17].

Atmospheric pollution is known to affect numerous physiological functions, including human reproduction and fertility, and it is reported to be related to lower semen quality [17–22], reduced fertility and spontaneous fertility rate [18–20], and reduced success rates of in vitro fertilisation (IVF) in humans [21,22]. Regarding the reprotoxicity of NMs, controversial reports have been published in recent years with particular attention to the effects on male gametes [23]. Few in vivo and in vitro studies have estimated the potential harmful impacts of CeO_2 NMs on reproductive organs and germ cells. Pristine CeO_2 NMs (5–40 nm) have been shown to cross the blood–testis barrier and accumulate in the testis (<0.2% of the inhaled dose) of rats following 28 days of inhalation in vivo (total estimated inhaled dose 0.83–4.24 mg/rat CeO_2 NMs) [24]. Accumulation of Ce in the testes of mice was also observed after 32 days of in vivo oral administration of pristine CeO_2 NMs (27.62 ± 3.01 nm) at the highest doses of 20 or 40 mg/kg body weight [25]. This accumulation caused a decrease in daily sperm production, lower motility, and sperm DNA damage [25]. Our team recently demonstrated the in vitro genotoxicity of pristine CeO_2 NMs (7 nm) on human sperm cells and mouse gametes after exposure to 10 μg$\cdot$L^{-1} [26,27]. Significant impairments in fertilisation rates were observed in mice [26], and a significant increase in DNA damage in human sperm [27]. The mechanisms of DNA damage were indirectly attributed to oxidative stress via the adjunction of an antioxidant (L-ergothineine) in the exposure medium [27].

Most of the previous studies were conducted with pristine CeO_2 NMs (i.e., at the production stage of the life cycle), which does not reflect a realistic exposure route of men and women to Ce-based NMs that are likely released in diesel exhaust. However, the WHO's International Agency for Research on Cancer classified diesel engine exhaust as carcinogenic to humans [28], and the OECD classified CeO_2 NMs as part of a priority list of NMs whose potential toxicity require urgent evaluation [16]. Hence, the potential reproductive toxicity [29] of combusted CeO_2 NMs must be evaluated.

This study was designed to evaluate the potential genotoxicity induced by in vitro exposure of human and rat sperm cells to low concentrations of combusted commercialised CeO_2 NM-based diesel additives (Envirox^{TM}). Combining biological assays with physico-chemical characterisation, we addressed two questions: (i) Do combusted CeO_2 NMs from a diesel additive induce genotoxic

effects towards human and rat sperm cells following in vitro exposure to low concentrations? (ii) Were the mechanisms of genotoxicity and the interactions with sperm cells different from pristine CeO_2 NMs?

2. Material and Methods

2.1. Physical-Chemical Characterisation

2.1.1. Ageing of the Diesel Fuel Additive

CeO_2 NMs were recovered from Envirox[TM], Energenics Europe Ltd., Oxfordshire, UK, which is a fuel-borne catalyst scientifically and commercially proven CeO_2 NM-based diesel additive supplied by Energenics Europe Ltd. Envirox[TM] was combusted following the protocol published in [4]. Briefly, we ultracentrifuged Envirox[TM] suspensions at $396,750\times g$ and $20\,^{\circ}C$ for 1 h and removed the supernatant to recover the pellet containing CeO_2 NMs. The pellets were freeze-dried (Heto PowerDry LL3000, Thermo Fisher Scientific, Strasbourg, France) for 5 days. The dried samples were crushed, and a total amount of 1.2 g was introduced in a furnace at $850\,^{\circ}C$ (i.e., at the average combustion temperature of diesel engines) [30] for 20 min. A stock suspension of the combusted Envirox[TM] (called aged CeO_2 NMs) was prepared in Milli-Q water at $10.15\,g{\cdot}L^{-1}$ of CeO_2. The combusted Envirox[TM] contained CeO_2 NMs with an average TEM size of 19 ± 10 nm, a larger polydispersity than the uncombusted ones, and a polyhedral shape [4]. We used X-ray diffraction (XRD) (X'Pert-Pro diffractometer, PANalytical) and transmission electron microscopy (TEM) (FEI 2Tecnaïi G2) to confirm the size, shape, and mineralogy of the produced NMs (see Supplementary Materials, Figure S1).

2.1.2. Aged CeO_2 NM Dissolution in FertiCult[®] Medium

We assessed the dissolution of aged CeO_2 NMs in FertiCult[®] medium (JCD Laboratories, Lyon, France) for the in vitro culture of mammalian gametes by inductively coupled plasma mass spectrometry (ICP-MS) (NexION 300X, Perkin Elmer[®]). We incubated aged CeO_2 NMs at room temperature (RT) in the culture medium for 2 and 5 h at three concentrations (10, 1000, and $100,000\,\mu g{\cdot}L^{-1}$). After incubation, the suspensions were ultra-filtered at 3 KDa (Amicon Ultra-15, Merck, France) at $3000\times g$ for 1 h and by ICP-MS; triplicates were performed for each concentration.

2.2. Gamete Collection

Rat sperm cell collection. After sacrifice, we collected and cut the epididymis to enable the exit of sperm in HTF-BSA culture medium (Human Tubal Fluid, Millipore[®], France, with 0.4% BSA: Bovine Serum Albumin, Sigma-Aldrich[®], Lyon, France) for 1 h at $37\,^{\circ}C$ and CO_2 5%.

Human sperm collection. We used frozen human sperm from healthy fertile donors. After thawing, we aliquoted the preparation and centrifuged it for 10 min at 420 g. The supernatants were discarded, and the pellets were exposed to various exposure conditions.

2.3. Ethical Authorization

Ethical authorization for animal sampling of gametes was obtained from the National Ethics Committee on Animal Experimentation (2018061110211950-V2 #15447). We used Sprague Dawley rats, Oncins France Strain A (623OFA), which were purchased from Charles River Laboratories, France. Sexually mature male rats of 60 days old were housed with free access to food and water until sacrifice.

Human sperm cells were purchased from GERMETHEQUE biobank, which obtained informed consent from each donor for inclusion of samples in the biobank and for their use in research experiments regarding human fertility in accordance with the 1975 Helsinki Declaration on human experimentation.

For oxidative stress analysis, the principle of Replacement of the 3R rule (reduction, refinement, and replacement) was applied and human sperm only was used.

2.4. Sperm Exposure

We exposed human and rat sperm to four different concentrations of aged CeO_2 NMs (1, 10, 100, and 1000 $\mu g \cdot L^{-1}$) for 1 h at 37 °C and 5% CO_2. FertiCult® medium was used as a negative control and 110 $\mu mol \cdot L^{-1}$ H_2O_2 as a positive control. The H_2O_2 concentration was chosen based on previous studies [26,27,31]. At least three different experiments were performed. After exposure, we recovered all motile sperm cells by swim-up [32], and before comet assay analysis, we measured sperm viability by eosin-nigrosine staining according to the World Health Organisation (WHO, 1999, Appendix IV.2) technique (100 cells were evaluated per condition).

2.5. DNA Damage Evaluation by Comet Assay

We performed the alkaline comet assay according to the procedure described by Singh [33] and adapted by Baumgartner [34], which has already been described in previous publications by our team [26,27,31]. DNA damage was quantified by the percentage of DNA in the tail of 100 randomly selected sperm cells from each triplicate slide per condition (at least 300 raw values analysed per experiment, at least 900 in total per condition).

Statistical Analysis. The data presented the medians of % Tail DNA values, with 1st and 3rd quartiles. We performed a linear mixed model analysis with "condition" (exposure condition) as a fixed effect and "cells" (sperm cells) within the replicate slide as a random effect using linear mixed effects regression (lmer) function of R software, version 3.6.0 (R Foundation for Statistical Computing, Vienna, Austria) to compare DNA damage among the various conditions. Pairwise differences of least-squares mean for all conditions were post-hoc assessed. Statistical significance was set at $p < 0.05$.

2.6. Oxidative Stress Analysis on Human Sperm

We investigated the effect on human sperm of aged CeO_2 NMs in vitro exposure on the generation of reactive oxygen species (ROS), at the exposure concentration that had induced the higher DNA damage, i.e., 1 $\mu g \cdot L^{-1}$. At least three different experiments were performed. We used a 2′,7′-dichlorodihydrofluorescein diacetate (H_2DCF-DA) probe [35]. The exposure protocol was readapted from Aitken et al. (2013) and Gallo et al. (2018) [36,37]. After thawing and dilution in FertiCult® culture medium, we centrifuged human sperm for 10 min at 420× g, discarded the supernatant and added 10 $\mu mol \cdot L^{-1}$ H_2DCF-DA [36] at 37 °C and 5% CO_2 for 45 min to enable internalization of the permeable probe. Then, the sperm cells were washed and exposed to 1 $\mu g \cdot L^{-1}$ CeO_2 NMs for 1 h at 37 °C and 5% CO_2. We used H_2O_2 110 $\mu mol \cdot L^{-1}$ as a positive control and FertiCult® medium as a negative control. After 1 h, we recovered the motile sperm by swim-up selection. For vitality staining, we exposed the sperm to 4′,6-diamidino-2-phenylindole (DAPI) at 0.5 $\mu g \cdot mL^{-1}$ immediately prior to analysis by flow cytometry (CytoFLEX, Beckman Coulter, IN, USA). The results are only based on a live sperm population and expressed as the percentage of DCF-positive cells (expressing the fluorescence) in 100,000 events per condition in each replicate experiment (300,000 live cells in total per condition).

2.7. Imaging of Human Sperm Cells after In Vitro Exposure

Human sperm were exposed in vitro to 1 and 100 $\mu g \cdot L^{-1}$ of aged CeO_2 NMs and selected by swim-up after 1 h. Non-exposed sperm cells were used as the control. Recovered motile sperm cells were washed with 0.1 M phosphate buffer, then fixed with glutaraldehyde 2.5% in 0.1 M phosphate buffer during 30 min at RT, and finally rinsed 3 times with 0.1 phosphate buffer. Samples were post-fixed with 2% osmium tetroxide in 0.1M phosphate buffer during 30 min and washed 3 times with 0.1 M phosphate buffer. Progressive dehydration with 50% to 100% Ethanol bath was performed before embedding in Epon 812 (epoxy resin) from 33% to 100% EPON. Ultrathin sections (60 nm) were obtained using Ultracut-E ultramicrotome (Reichert-Jung, Southbridge, MA, USA) and contrast was performed using Uranyl acetate 5% for 12 min and dried at room temperature. Pictures were obtained

using a JEM 1400 transmission electron microscope (JEOL, Tokyo, Japan) at 80 kV with a Megaview III camera under iTEM Five software (SIS Imaging, Münster, Germany). This procedure was described in [27].

3. Results

3.1. No Detectable Dissolution of Aged CeO$_2$ NMs in Abiotic Conditions

The dissolution (<3 kDa) of CeO$_2$ NMs in abiotic FertiCult$^®$ medium (pH 7.2–7.5) was studied after 2 and 5 h of incubation at 10, 1000, and 100,000 µg·L^{-1}. Regardless of the concentrations tested, no dissolution of the CeO$_2$ NMs could be measured by ICP-MS in abiotic conditions. Below 3 kDa, the concentrations of dissolved Ce species were under the limits of detection (i.e., <0.002 µg·L^{-1}).

3.2. Higher DNA Damage Detected at the Lowest Concentration Exposure

Rat and human sperm cells were exposed in vitro for one hour to 0, 1, 10, 100, or 1000 µg·L^{-1} of aged CeO$_2$ NMs. After exposure, all viability rates exceeded the normality threshold as stated by the WHO criteria [38]. The results are presented as the distribution of median values of % tail DNA with 1st and 3rd quartiles, obtained from 3 independent experiments. $p < 0.05$, for the differences compared versus *: negative control (NEG), a: vs. 10 µg·L^{-1} CeO$_2$ NMs, b: vs. 100 µg·L^{-1} CeO$_2$ NMs, c: vs. 1000 µg·L^{-1} CeO$_2$ NMs (Figure 1a,b).

(**a**)   (**b**)
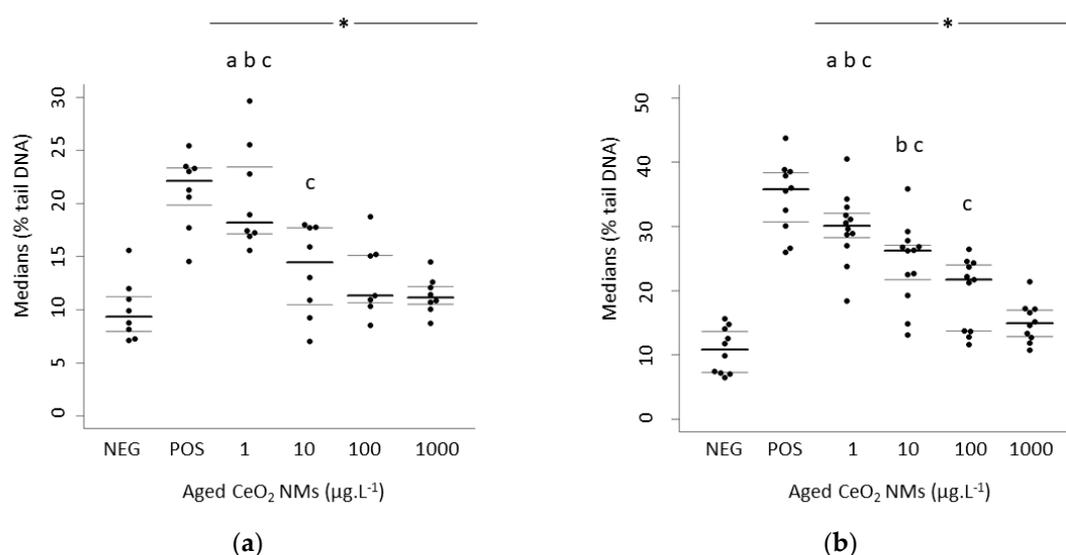
Figure 1. Evaluation of DNA damage using the Comet Assay following in vitro exposure of rat (**a**) and human sperm (**b**) to aged CeO$_2$ NMs. Tested concentrations: 0, 1, 10, 100, and 1000 µg·L^{-1} of aged CeO$_2$ NMs, POS (110 µM H$_2$O$_2$, positive control). $p < 0.05$, for differences compared versus *: negative control (NEG); a: vs. 10 µg·L^{-1} CeO$_2$ NMs; b: vs. 100 µg·L^{-1} CeO$_2$ NMs; c: vs. 1000 µg·L^{-1} CeO$_2$ NMs. In each condition, the main central line corresponds to the median of the points and the two other lines correspond to 1st and 3rd quartiles.

In rat- and human-exposed sperm cells, all exposure concentrations induced significantly higher DNA damage than the negative control ($p < 0.05$) (Figure 1a,b). Furthermore, a significant increase in DNA damage was observed at the lowest tested concentration (1 µg·L^{-1}) (medians of % tail DNA in rats and humans of 18.20 and 30.10, respectively) compared to the exposure to 10, 100, and 1000 µg·L^{-1} aged CeO$_2$ NMs; ($p < 0.001$). We also observed a significant difference between 10 and 1000 µg·L^{-1} aged CeO$_2$ NMs in rat sperm ($p < 0.05$) and a significant difference among the three highest tested concentrations in human sperm ($p < 0.05$). The variability of biological data in the 3 independent experiments is presented in Table 1.

Table 1. Biological variability of the data. Median values of % Tail DNA of each condition of three experiments, with 1st and 3rd quartiles.

Rat Sperm Cells	MEDIAN Values	1st Quartile	3rd Quartile	Human Sperm Cells	MEDIAN values	1st Quartile	3rd Quartile
Negative control	9.34	7.94	11.24	Negative control	10.8	7.26	13.7
1 $\mu g \cdot L^{-1}$ CeO_2	18.2	17.17	23.47	1 $\mu g \cdot L^{-1}$ CeO_2	30.1	28.28	32.06
10 $\mu g \cdot L^{-1}$ CeO_2	14.46	10.48	17.72	10 $\mu g \cdot L^{-1}$ CeO_2	26.24	21.69	27.09
100 $\mu g \cdot L^{-1}$ CeO_2	11.31	10.64	15.13	100 $\mu g \cdot L^{-1}$ CeO_2	21.74	13.72	23.99
1000 $\mu g \cdot L^{-1}$ CeO_2	11.15	10.53	12.19	1000 $\mu g \cdot L^{-1}$ CeO_2	14.91	12.88	17.02

3.3. Oxidative Stress Detected in Human Sperm

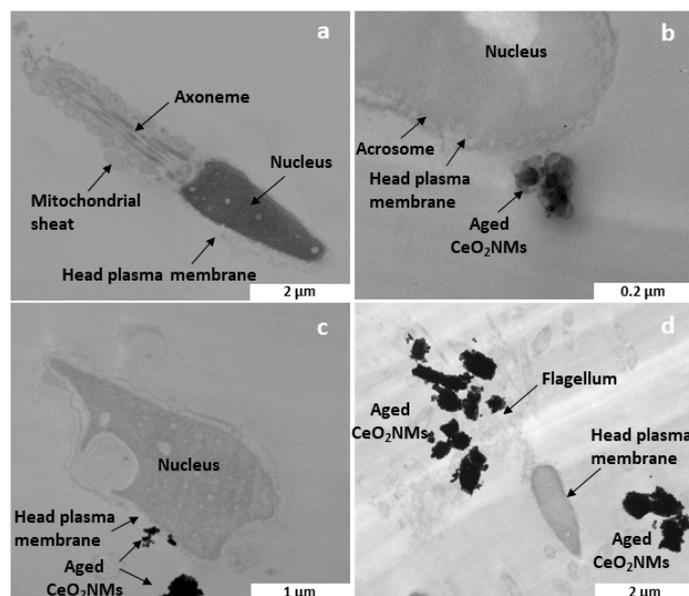After 1 h of in vitro exposure to 1 $\mu g \cdot L^{-1}$ aged CeO_2 NMs, the percentage of DCF-positive live sperm (mean ± SEM= 13.1 ± 3.9) significantly increased compared to the negative control (5.21 ± 2.9) ($p = 0.047$) (Figure 2).
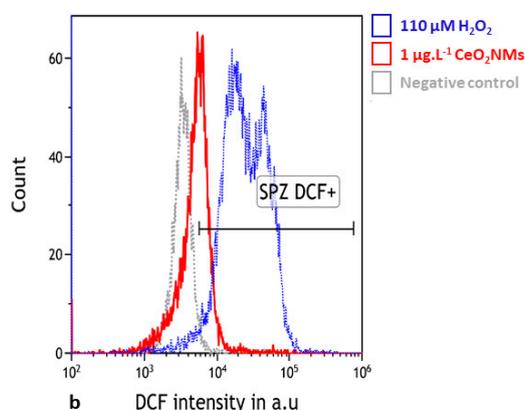
Figure 2. Detection of reactive oxygen species (ROS) using the H_2DCF-DA probe. Human sperm cells were exposed in vitro for one hour to 1 $\mu g \cdot L^{-1}$ aged CeO_2 NMs. Intracellular reactive oxygen species were evaluated by the dichlorodihydrofluorescein (DCF) intensity. The results are representative of 3 independent experiments. $p < 0.05$, for differences compared versus negative control. SPZ: spermatozoa. a.u: arbitrary unit.

3.4. Aged CeO_2 NMs Detected by TEM on the Plasma Membrane of Human Sperm

In human sperm cells, TEM detected aged CeO_2 NM aggregates near the sperm plasma membrane after the exposure to 1 $\mu g \cdot L^{-1}$ CeO_2 NMs (Figure 3b,c). After the exposure to 100 $\mu g \cdot L^{-1}$, the NMs appeared even more aggregated and not in close interaction with the cells (Figure 3d). No CeO_2 NM internalization was observed by TEM at any exposure concentration.

Figure 3. TEM analysis of aged CeO_2 NMs in human sperm after in vitro exposure. (**a**) negative control; (**b**,**c**) exposed to 1 μg·L^{-1} CeO_2 NMs; (**d**): exposed to 100 μg·L^{-1} CeO_2 NMs. The white rectangles correspond to the scale bar.

4. Discussion

4.1. Exposure to Low Doses of Aged CeO_2 NMs Induced Higher DNA Damage

One major drawback of the currently used studies and models to evaluate the toxicity of NMs for humans is the lack of relevance of the exposure scenario (i.e., relevant concentration of NMs, relevant speciation of the tested NMs) [39]. Indeed, most in vivo studies are based on theoretical data regarding the potential exposure of humans to CeO_2 NMs. For example, Modrzynska (2018) exposed mice to a single dose of 162 μg of CeO_2 or TiO_2 NMs in 50 μL of 2% serum in nano-pure water [40]. This single dose corresponds to pulmonary deposition during 138-h working days at the Danish occupational exposure limit of 10 mg/m^3 for TiO_2 assuming 9% alveolar deposition [41,42]. Li (2016) exposed rats to CeO_2 NMs in a nose-only exposure system for a single 4-h exposure (27–39.8 μg/m^3). They used a scanning mobility particle sizer to estimate the average mass concentration and compared it with the physical sampling measurements based on the filter packs [43].

Here, we highlighted the importance of the dose and more particularly of the low dose. We expected a moderate release of CeO_2 NMs in the air from a diesel engine and a spread into the gonads, as shown by Qin et al. (2019) and Préaubert et al. (2015) [25,26]. The lowest concentration of aged CeO_2 NMs (1 μg·L^{-1}) was found to induce the highest DNA damage in both human and rat sperm cells (Figure 1a,b). These results are consistent with our previous study, which showed inverse dose-response DNA damage after the in vitro exposure of human sperm to pristine CeO_2 NMs [27]. Few hypotheses could be formulated to explain the highest genotoxicity at the lowest exposure concentration. One refers to different NMs/cells interactions because of dose-dependent aggregation states. Herein, it was not technically possible (below the detection limit) to measure the size of NMs aggregates at 1 μg·L^{-1} and 1000 μg·L^{-1} of CeO_2 NMs in the FertiCult® medium. However, the strong aggregation due to combustion already observed in reference [4] is also expected at the pH and ionic strength of extracellular media. Based on the dose-dependent probability of contact between NMs, smaller aggregates should be expected at the lowest concentration (1 μg·L^{-1} CeO_2). In that case, smaller aggregates would be more prone to interact with the cells and enhance their biotransformation, biological, and toxicological effects [44]. It is known that nanoparticle genotoxicity and cytotoxicity are controversial, especially because these interactions are species-specific, often tissue-specific, and related

to physico-chemical features of exposure medium [45,46]. Moreover, nanoparticles show a strong tendency to form agglomerates in solution due to their high surface area. It is a general opinion that the degree and type of agglomerates formed may influence the toxicity of NPs [47,48].

4.2. DNA Damage in Human Sperm Was Associated with Oxidative Stress

A generally accepted paradigm is that the toxicity of NMs arises primarily because they can generate reactive oxygen species (ROS) and oxidative damage [44]. Oxidative stress is a major cause of DNA damage in mammalian spermatozoa [49], since it can affect the membrane integrity and motility [50,51], and it is also associated with failures of fertilisation, abnormal embryonic development, and premature pregnancy loss [52].

Understanding the mechanism of action of CeO_2 NMs is a major challenge since they are known to exhibit pro- and antioxidant properties. For example, Das et al. (2007) [53] and Niu et al. (2007) [54] showed that CeO_2 NMs (3–5 and 7 nm, respectively) could reduce oxidative stress as free radical scavengers, whereas Auffan et al. (2009) [55] highlighted the ability of CeO_2 NMs (7 nm) to damage fibroblast DNA at very low doses (6–1.2×10^6 $\mu g \cdot L^{-1}$). The determining factors are the stoichiometry, oxido-reduction state of Ce, pH of the medium, presence of H_2O_2, etc. [56], but it also depends on the cell types, organisms [57], size and speciation of the NMs [58].

Herein, we demonstrated in human sperm that 1 h of in vitro exposure to 1 $\mu g \cdot L^{-1}$ aged CeO_2 NMs induced a significant increase in ROS generation. The H_2DCF-DA probe becomes fluorescent on oxidation and is purported to directly monitor reactive oxygen and/or nitrogen species (ROS/RNS) [59]. ONOO- and the hydroxyl radical also directly oxidise this probe and significantly contribute to the positive signals observed in defective human spermatozoa [60,61]. Our results confirm previous studies, where we showed that DNA damage was induced in human sperm by exposure to 10 $\mu g \cdot L^{-1}$ of pristine CeO_2 NMs was significantly decreased by the addition of an antioxidant (L-ergothioneine) in the exposure medium [27]. L-ergothioneine is known to scavenge hydroxyl radicals, hypochlorous acid, and peroxynitrite [62], which can directly oxidise the H_2DCF-DA probes [60,61]. We hypothesize that oxidative stress can be one of the mechanisms responsible for the DNA damage detected in sperm cells.

At 1 $\mu g \cdot L^{-1}$, aged CeO_2 NMs were found in close contact with the plasma membrane of the head of the spermatozoa. This interaction with the sperm head associated with the highest sensitivity of the H_2DCF-DA probe when oxidants are generated near the plasma membrane or in the cytoplasm [36] can help us elucidate the mechanisms of oxidative stress generated by aged CeO_2 NMs. Indeed, the head of the spermatozoa expresses various ion channels (e.g., Ca^{2+} and K^+) [63,64], which offer entry paths for metallic toxicants such as Zn^{2+} and Pb^{2+} into a mature spermatozoa [63,65,66]. More interestingly, some trivalent ions such as La^{3+} and Ce^{3+} act as T-type calcium channel antagonists and competitively bind and block the Ca^{2+} binding sites [67,68], which are required for the sperm head mannose receptors [65]. Then, mannose receptor expression is considered a biomarker for the effects of transition and heavy metals and organic toxicants on sperm fertility potential [66].

Here, we did not observe any abiotic dissolution of Ce in the Ferticult® medium. However, reductive dissolution of nanocrystalline Ce(IV)O_2 into Ce(III) is pH-dependent at pH < 7 [69–71] and it is possible that a release of Ce(III) with a pro-oxidant activity could occur in the vicinity of the cells due to the metabolic activity [69,70]. Indeed, in sperm cells, voltage-gated proton channels Hv1 (i.e., the main H(+) extrusion pathway) activated by alkaline extracellular environment induce an alkalinisation of intracellular pH necessary for the functional activation (capacitation) of sperm, and consequently a decrease in extracellular pH [72]. Such an extracellular pH decrease could locally enhance the dissolution of CeO_2 NMs in the vicinity of the cells. More information on the biodistribution and biotransformation of CeO_2 at the scale of the cell membrane is required to validate the hypothesis that the observed oxidative stress can be attributed to the possible biotransformation of CeO_2 at the surface of the plasma membrane.

4.3. Lifecycle Stage-Dependent (Geno)Toxicity of CeO_2 NMs

To date, few studies have explored the DNA damage and oxidative stress induced by pristine CeO_2 NMs (mostly monodisperse and homogeneously coated), which are not representative of CeO_2 NMs that are likely released during use. One strength of this study is the use of combusted Envirox[TM] to mimic real exposure to CeO_2 NMs, which are potentially released from diesel vehicles equipped with an active nano-catalyst for soot abatement. With an over-combustion in a single-cylinder engine with mechanical fuel injection [13] or in an oven at a temperature close to that of diesel engines [4], the physico-chemical properties of CeO_2 NMs evolve compared to those initially incorporated in the diesel additive: the size of the CeO_2 crystallites significantly increased (i.e., the decrease in specific surface area from 113 ± 17 to 63 ± 35 $m^2 \cdot g^{-1}$) without detectable Ce(III) in the structure, and no organic compounds remained at the surface. This transformation upon combustion highlights that at each stage of the nano-enabled product life cycle (formulation, usage/combustion, and end of life), the mechanisms and kinetics of interactions between the released CeO_2 NMs and the aqueous media (e.g., water, soil, biological media) and exposed organisms will differ [5,73]. Hence, the life cycle stages of nano-enabled products when studying their toxicity is critical [62,74]. This is particularly the case when studying their genotoxicology [75] towards gametes since fertility may be altered, which subsequently affects the reproduction rate and health of the offspring [26,76].

Based on previously published data and the current study, we compared the impacts towards gametes of pristine CeO_2 NMs (production stage of the life cycle) and combusted diesel additives (usage stage of the lifecycle). At both lifecycle stages, a higher genotoxicity attributed to oxidative stress was observed at the lowest doses towards human sperm cells [26,27]. For pristine and combusted NMs, an inverse dose–effect relationship was attributed to different aggregation states (size and density). At low doses, the probability of contact between two particles (homo-aggregation) decreases, and CeO_2 NMs are likely more dispersed, which increases the contact surface between NMs and cells [27]. However, for pristine NMs only, the significant genotoxicity at low doses was also attributed to their chemical instability because of their larger specific surface area and an organic coating at the surface [4].

5. Conclusions

We demonstrated for the first time the DNA damage induced in human and rat sperm cells after exposure to low concentrations of CeO_2 NMs, which are similar to the ones released by combustion in a diesel engine. In vitro exposure to the lowest concentration of combusted CeO_2 NM induced oxidative stress in human sperm cells after the interaction with the plasma membrane. While important from a mechanistic standpoint, this study remains limited by its in vitro nature. However, in vitro exposure is a relevant design since spermatozoa can encounter nanoparticles in the male gonads or female genital tract. In vivo studies after a low-dose exposure to aged NMs will help us more closely approach realistic exposure conditions. Then, we will be able to decipher the transfer of CeO_2 NMs at different stages of the lifecycle to various organs in animals, their permeation of biological membranes, accumulation in reproductive organs, and their impact on embryonic development, as conducted with pristine NMs [67,77–80]. To go further in the relevance of the exposure scenario, the complexity of the exhaust emissions [81] should be considered when assessing their genotoxicity. For instance, a considerable amount of Polycyclic Aromatic Hydrocarbons (PAHs) and their alkylated derivatives are emitted by diesel engines [82]. Some of them are well known for their carcinogenic and reprotoxic potential, such as benzo[a]pyrene (B*a*P) [83]. An even more relevant exposure scenario can assess the potential hazard due to co-exposure to combusted CeO_2 NMs associated with other organic compounds generated during diesel combustion.

Supplementary Materials: The following are available online at http://www.mdpi.com/2079-4991/10/12/2327/s1. Figure S1: X-ray diffractogram and transmission electron microscopy image of the 850 °C aged CeO_2 NMs.

References

1. Lee, J.; Jeong, J.-S.; Kim, S.Y.; Lee, S.-J.; Shin, Y.-J.; Im, W.-J.; Kim, S.-H.; Park, K.; Jeong, E.J.; Nam, S.-Y.; et al. Safety assessment of cerium oxide nanoparticles: Combined repeated-dose toxicity with reproductive/developmental toxicity screening and biodistribution in rats. *Nanotoxicology* **2020**, 1–15. [CrossRef] [PubMed]

2. Oberdörster, G.; Oberdörster, E.; Oberdörster, J. Nanotoxicology: An Emerging Discipline Evolving from Studies of Ultrafine Particles. *Environ. Health Perspect.* **2005**, *113*, 823–839. [CrossRef] [PubMed]

3. Graczyk, H.; Riediker, M. Occupational exposure to inhaled nanoparticles: Are young workers being left in the dust? *J. Occup. Health* **2019**, *61*, 333–338. [CrossRef] [PubMed]

4. Auffan, M.; Tella, M.; Liu, W.; Pariat, A.; Cabié, M.; Borschneck, D.; Angeletti, B.; Landrot, G.; Mouneyrac, C.; Giambérini, L.; et al. Structural and physical–chemical behavior of a CeO_2 nanoparticle based diesel additive during combustion and environmental release. *Environ. Sci. Nano* **2017**, *4*, 1974–1980. [CrossRef]

5. Masion, A.; Auffan, M.; Rose, J. Monitoring the Environmental Aging of Nanomaterials: An Opportunity for Mesocosm Testing? *Materials* **2019**, *12*, 2447. [CrossRef] [PubMed]

6. Gaiser, B.K.; Fernandes, T.F.; Jepson, M.; Lead, J.R.; Tyler, C.R.; Stone, V. Assessing exposure, uptake and toxicity of silver and cerium dioxide nanoparticles from contaminated environments. *Environ. Health* **2009**, *8*, S2. [CrossRef] [PubMed]

7. Park, B.; Martin, P.; Harris, C.; Guest, R.; Whittingham, A.; Jenkinson, P.; Handley, J. Initial in vitro screening approach to investigate the potential health and environmental hazards of Envirox™—A nanoparticulate cerium oxide diesel fuel additive. *Part. Fibre Toxicol.* **2007**, *4*, 12. [CrossRef]

8. Jung, H.; Kittelson, D.B. Measurement of Electrical Charge on Diesel Particles. *Aerosol Sci. Technol.* **2005**, *39*, 1129–1135. [CrossRef]

9. Zhang, J.; Nazarenko, Y.; Zhang, L.; Calderon, L.; Lee, K.-B.; Garfunkel, E.; Schwander, S.; Tetley, T.D.; Chung, K.F.; Porter, A.E.; et al. Impacts of a Nanosized Ceria Additive on Diesel Engine Emissions of Particulate and Gaseous Pollutants. *Environ. Sci. Technol.* **2013**, *47*, 13077–13085. [CrossRef]

10. Park, B.; Donaldson, K.; Duffin, R.; Tran, L.; Kelly, F.; Mudway, I.; Morin, J.-P.; Guest, R.; Jenkinson, P.; Samaras, Z.; et al. Hazard and Risk Assessment of a Nanoparticulate Cerium Oxide-Based Diesel Fuel Additive—A Case Study. *Inhal. Toxicol.* **2008**, *20*, 547–566. [CrossRef]

11. Johnson, A.C.; Park, B. Predicting contamination by the fuel additive cerium oxide engineered nanoparticles within the United Kingdom and the associated risks. *Environ. Toxicol. Chem.* **2012**, *31*, 2582–2587. [CrossRef] [PubMed]

12. Gantt, B.; Hoque, S.; Willis, R.D.; Fahey, K.M.; Delgado-Saborit, J.M.; Harrison, R.M.; Erdakos, G.B.; Bhave, P.V.; Zhang, K.M.; Kovalcik, K.; et al. Near-Road Modeling and Measurement of Cerium-Containing Particles Generated by Nanoparticle Diesel Fuel Additive Use. *Environ. Sci. Technol.* **2014**, *48*, 10607–10613. [CrossRef] [PubMed]

13. Batley, G.E.; Halliburton, B.; Kirby, J.K.; Doolette, C.L.; Navarro, D.; McLaughlin, M.J.; Veitch, C. Characterization and ecological risk assessment of nanoparticulate CeO_2 as a diesel fuel catalyst: Characterization and risk of nano-CeO_2 as a diesel catalyst. *Environ. Toxicol. Chem.* **2013**, *32*, 1896–1905. [CrossRef] [PubMed]

14. Dale, J.G.; Cox, S.S.; Vance, M.E.; Marr, L.C.; Hochella, M.F. Transformation of Cerium Oxide Nanoparticles from a Diesel Fuel Additive during Combustion in a Diesel Engine. *Environ. Sci. Technol.* **2017**, *51*, 1973–1980. [CrossRef] [PubMed]

15. Cassee, F.R.; van Balen, E.C.; Singh, C.; Green, D.; Muijser, H.; Weinstein, J.; Dreher, K. Exposure, Health and Ecological Effects Review of Engineered Nanoscale Cerium and Cerium Oxide Associated with its Use as a Fuel Additive. *Crit. Rev. Toxicol.* **2011**, *41*, 213–229. [CrossRef] [PubMed]

16. OECD's Guidelines OECD's Meeting on Safety Testing of Manufactured Nanomaterials and Test Guidelines. March 2011. Available online: http://www.oecd.org/science/nanosafety/48291037.pdf (accessed on 15 May 2020).

17. Haase, A.; Luch, A. Genotoxicity of nanomaterials in vitro: Treasure or trash? *Arch. Toxicol.* **2016**, *90*, 2827–2830. [CrossRef] [PubMed]

18. Dejmek, J.; Jelínek, R.; Solansky', I.; Benes, I.; Srám, R.J. Fecundability and parental exposure to ambient sulfur dioxide. *Environ. Health Perspect.* **2000**, *108*, 647–654. [CrossRef]

19. Nieuwenhuijsen, M.J.; Basagaña, X.; Dadvand, P.; Martinez, D.; Cirach, M.; Beelen, R.; Jacquemin, B. Air pollution and human fertility rates. *Environ. Int.* **2014**, *70*, 9–14. [CrossRef]

20. Slama, R.; Bottagisi, S.; Solansky, I.; Lepeule, J.; Giorgis-Allemand, L.; Sram, R. Short-Term Impact of Atmospheric Pollution on Fecundability. *Epidemiology* **2013**, *24*, 871–879. [CrossRef]

21. Legro, R.S.; Sauer, M.V.; Mottla, G.L.; Richter, K.S.; Li, X.; Dodson, W.C.; Liao, D. Effect of air quality on assisted human reproduction. *Hum. Reprod.* **2010**, *25*, 1317–1324. [CrossRef]

22. Perin, P.M.; Maluf, M.; Czeresnia, C.E.; Nicolosi Foltran Januário, D.A.; Nascimento Saldiva, P.H. Effects of exposure to high levels of particulate air pollution during the follicular phase of the conception cycle on pregnancy outcome in couples undergoing in vitro fertilization and embryo transfer. *Fertil. Steril.* **2010**, *93*, 301–303. [CrossRef] [PubMed]

23. Falchi, L.; Khalil, W.A.; Hassan, M.; Marei, W.F.A. Perspectives of nanotechnology in male fertility and sperm function. *Int. J. Vet. Sci. Med.* **2018**, *6*, 265–269. [CrossRef] [PubMed]

24. Geraets, L.; Oomen, A.G.; Schroeter, J.D.; Coleman, V.A.; Cassee, F.R. Tissue Distribution of Inhaled Micro- and Nano-sized Cerium Oxide Particles in Rats: Results From a 28-Day Exposure Study. *Toxicol. Sci.* **2012**, *127*, 463–473. [CrossRef] [PubMed]

25. Qin, F.; Shen, T.; Li, J.; Qian, J.; Zhang, J.; Zhou, G.; Tong, J. SF-1 mediates reproductive toxicity induced by Cerium oxide nanoparticles in male mice. *J. Nanobiotechnol.* **2019**, 17. [CrossRef] [PubMed]

26. Préaubert, L.; Courbiere, B.; Achard, V.; Tassistro, V.; Greco, F.; Orsiere, T.; Bottero, J.-Y.; Rose, J.; Auffan, M.; Perrin, J. Cerium dioxide nanoparticles affect in vitro fertilization in mice. *Nanotoxicology* **2015**, *10*, 111–117. [CrossRef] [PubMed]

27. Préaubert, L.; Tassistro, V.; Auffan, M.; Sari-Minodier, I.; Rose, J.; Courbiere, B.; Perrin, J. Very low concentration of cerium dioxide nanoparticles induce DNA damage, but no loss of vitality, in human spermatozoa. *Toxicol. In Vitro* **2018**, *50*, 236–241. [CrossRef]

28. Benbrahim-Tallaa, L.; Baan, R.A.; Grosse, Y.; Lauby-Secretan, B.; El Ghissassi, F.; Bouvard, V.; Guha, N.; Loomis, D.; Straif, K. Carcinogenicity of diesel-engine and gasoline-engine exhausts and some nitroarenes. *Lancet Oncol.* **2012**, *13*, 663–664. [CrossRef]

29. OECD's Guidelines, Report of the OECD Expert Meeting on the Physical Chemical Properties of Manufactured Nanomaterials and Test Guidelines 2014. Available online: http://www.oecd.org/env/ehs/nanosafety/publications-series-safety-manufactured-nanomaterials.htm (accessed on 15 May 2020).

30. Flynn, P.F.; Durrett, R.P.; Hunter, G.L.; zur Loye, A.O.; Akinyemi, O.C.; Dec, J.E.; Westbrook, C.K. *Diesel Combustion: An Integrated View Combining Laser Diagnostics, Chemical Kinetics, and Empirical Validation*; SAE International: Warrendale, PA, USA, 1999.

31. Einaudi, L.; Courbiere, B.; Tassistro, V.; Prevot, C.; Sari-Minodier, I.; Orsiere, T.; Perrin, J. In vivo exposure to benzo(a)pyrene induces significant DNA damage in mouse oocytes and cumulus cells. *Hum. Reprod.* **2014**, *29*, 548–554. [CrossRef]

32. Perrin, J.; Tassistro, V.; Mandon, M.; Grillo, J.-M.; Botta, A.; Sari-Minodier, I. Tobacco consumption and benzo(a)pyrene-diol-epoxide-DNA adducts in spermatozoa: In smokers, swim-up procedure selects spermatozoa with decreased DNA damage. *Fertil. Steril.* **2011**, *95*, 2013–2017. [CrossRef]

33. Singh, N.P.; McCoy, M.T.; Tice, R.R.; Schneider, E.L. A simple technique for quantitation of low levels of DNA damage in individual cells. *Exp. Cell Res.* **1988**, *175*, 184–191. [CrossRef]

34. Baumgartner, A.; Cemeli, E.; Anderson, D. The comet assay in male reproductive toxicology. *Cell Biol. Toxicol.* **2009**, *25*, 81–98. [CrossRef] [PubMed]

35. Chen, X.; Zhong, Z.; Xu, Z.; Chen, L.; Wang, Y. 2′,7′-Dichlorodihydrofluorescein as a fluorescent probe for reactive oxygen species measurement: Forty years of application and controversy. *Free Radic. Res.* **2010**, *44*, 587–604. [CrossRef] [PubMed]

36. Aitken, R.J.; Smith, T.B.; Lord, T.; Kuczera, L.; Koppers, A.J.; Naumovski, N.; Connaughton, H.; Baker, M.A.; De Iuliis, G.N. On methods for the detection of reactive oxygen species generation by human spermatozoa: Analysis of the cellular responses to catechol oestrogen, lipid aldehyde, menadione and arachidonic acid. *Andrology* **2013**, *1*, 192–205. [CrossRef] [PubMed]

37. Gallo, A.; Manfra, L.; Boni, R.; Rotini, A.; Migliore, L.; Tosti, E. Cytotoxicity and genotoxicity of CuO nanoparticles in sea urchin spermatozoa through oxidative stress. *Environ. Int.* **2018**, *118*, 325–333. [CrossRef]

38. *WHO Laboratory Manual for the Examination and Processing of Human Semen*, 5th ed.; World Health Organization: Geneva, Switzerland, 2010; ISBN 978-92-4-154778-9.

39. Kuhlbusch, T.A.J. Nanomaterial exposures for worker, consumer and the general public. *NanoImpact* **2018**, *10*, 11–25. [CrossRef]

40. Modrzynska, J.; Berthing, T.; Ravn-Haren, G.; Kling, K.; Mortensen, A.; Rasmussen, R.R.; Larsen, E.H.; Saber, A.T.; Vogel, U.; Loeschner, K. In vivo-induced size transformation of cerium oxide nanoparticles in both lung and liver does not affect long-term hepatic accumulation following pulmonary exposure. *PLoS ONE* **2018**, *13*, e0202477. [CrossRef]

41. Hougaard, K.S.; Jackson, P.; Jensen, K.A.; Sloth, J.J.; Löschner, K.; Larsen, E.H.; Birkedal, R.K.; Vibenholt, A.; Boisen, A.-M.Z.; Wallin, H.; et al. Effects of prenatal exposure to surface-coated nanosized titanium dioxide (UV-Titan). A study in mice. *Part. Fibre Toxicol.* **2010**, *7*, 16. [CrossRef]

42. Jacobsen, N.R.; Møller, P.; Jensen, K.A.; Vogel, U.; Ladefoged, O.; Loft, S.; Wallin, H. Lung inflammation and genotoxicity following pulmonary exposure to nanoparticles in ApoE$^{-/-}$ mice. *Part. Fibre Toxicol.* **2009**, *6*, 2. [CrossRef]

43. Li, D.; Morishita, M.; Wagner, J.G.; Fatouraie, M.; Wooldridge, M.; Eagle, W.E.; Barres, J.; Carlander, U.; Emond, C.; Jolliet, O. In vivo biodistribution and physiologically based pharmacokinetic modeling of inhaled fresh and aged cerium oxide nanoparticles in rats. *Part. Fibre Toxicol.* **2016**, *13*, 45. [CrossRef]

44. Fu, P.P.; Xia, Q.; Hwang, H.-M.; Ray, P.C.; Yu, H. Mechanisms of nanotoxicity: Generation of reactive oxygen species. *J. Food Drug Anal.* **2014**, *22*, 64–75. [CrossRef]

45. Rocco, L.; Santonastaso, M.; Mottola, F.; Costagliola, D.; Suero, T.; Pacifico, S.; Stingo, V. Genotoxicity assessment of TiO$_2$ nanoparticles in the teleost *Danio rerio*. *Ecotoxicol. Environ. Saf.* **2015**, *113*, 223–230. [CrossRef] [PubMed]

46. Mottola, F.; Iovine, C.; Santonastaso, M.; Romeo, M.L.; Pacifico, S.; Cobellis, L.; Rocco, L. NPs-TiO$_2$ and Lincomycin Coexposure Induces DNA Damage in Cultured Human Amniotic Cells. *Nanomaterials* **2019**, *9*, 1511. [CrossRef] [PubMed]

47. Mohanraj, V.J.; Chen, Y. Nanoparticles—A review. *Trop. J. Pharm. Res.* **2006**, *5*, 561–573. [CrossRef]

48. Sager, T.M.; Porter, D.W.; Robinson, V.A.; Lindsley, W.G.; Schwegler-Berry, D.E.; Castranova, V. Improved method to disperse nanoparticles for in vitro and in vivo investigation of toxicity. *Nanotoxicology* **2007**, *1*, 118–129. [CrossRef]

49. Aitken, R.J. Reactive oxygen species as mediators of sperm capacitation and pathological damage. *Mol. Reprod. Dev.* **2017**, *84*, 1039–1052. [CrossRef]

50. Agarwal, A. Oxidative Stress and Male Infertility: From Research Bench to Clinical Practice. *J. Androl.* **2002**, *23*, 737–752. [CrossRef]

51. Aitken, R.J.; Gordon, E.; Harkiss, D.; Twigg, J.P.; Milne, P.; Jennings, Z.; Irvine, D.S. Relative Impact of Oxidative Stress on the Functional Competence and Genomic Integrity of Human Spermatozoa. *Biol. Reprod.* **1998**, *59*, 1037–1046. [CrossRef]

52. Aitken, R.J.; Curry, B.J. Redox regulation of human sperm function: From the physiological control of sperm capacitation to the etiology of infertility and DNA damage in the germ line. *Antioxid. Redox Signal.* **2011**, *14*, 367–381. [CrossRef]

53. Das, M.; Patil, S.; Bhargava, N.; Kang, J.-F.; Riedel, L.M.; Seal, S.; Hickman, J.J. Auto-catalytic Ceria Nanoparticles Offer Neuroprotection to Adult Rat Spinal Cord Neurons. *Biomaterials* **2007**, *28*, 1918–1925. [CrossRef]

54. Niu, J.; Azfer, A.; Rogers, L.M.; Wang, X.; Kolattukudy, P.E. Cardioprotective effects of cerium oxide nanoparticles in a transgenic murine model of cardiomyopathy. *Cardiovasc. Res.* **2007**, *73*, 549–559. [CrossRef]

55. Auffan, M.; Rose, J.; Wiesner, M.R.; Bottero, J.-Y. Chemical stability of metallic nanoparticles: A parameter controlling their potential cellular toxicity in vitro. *Environ. Pollut.* **2009**, *157*, 1127–1133. [CrossRef] [PubMed]

56. Sozarukova, M.M.; Proskurnina, E.V.; Baranchikov, A.E.; Ivanov, V.K. CeO_2 nanoparticles as free radical regulators in biological systems. *Nanosyst. Phys. Chem. Math.* **2020**, *11*, 324–332. [CrossRef]

57. Pulido-Reyes, G.; Rodea-Palomares, I.; Das, S.; Sakthivel, T.S.; Leganes, F.; Rosal, R.; Seal, S.; Fernández-Piñas, F. Untangling the biological effects of cerium oxide nanoparticles: The role of surface valence states. *Sci. Rep.* **2015**, *5*. [CrossRef] [PubMed]

58. Hayes, S.A.; Yu, P.; O'Keefe, T.J.; O'Keefe, M.J.; Stoffer, J.O. The Phase Stability of Cerium Species in Aqueous Systems. Part 1. E-pH Diagram for the Ce—$HClO_4$—H_2O System. *ChemInform* **2002**, *34*. [CrossRef]

59. Guo, T.; Cui, L.; Shen, J.; Wang, R.; Zhu, W.; Xu, Y.; Qian, X. A dual-emission and large Stokes shift fluorescence probe for real-time discrimination of ROS/RNS and imaging in live cells. *Chem. Commun.* **2013**, *49*, 1862. [CrossRef] [PubMed]

60. Myhre, O.; Andersen, J.M.; Aarnes, H.; Fonnum, F. Evaluation of the probes 2′,7′-dichlorofluorescin diacetate, luminol, and lucigenin as indicators of reactive species formation. *Biochem. Pharmacol.* **2003**, *65*, 1575–1582. [CrossRef]

61. Mahfouz, R.; Sharma, R.; Lackner, J.; Aziz, N.; Agarwal, A. Evaluation of chemiluminescence and flow cytometry as tools in assessing production of hydrogen peroxide and superoxide anion in human spermatozoa. *Fertil. Steril.* **2009**, *92*, 819–827. [CrossRef]

62. Tang, R.M.Y.; Cheah, I.K.-M.; Yew, T.S.K.; Halliwell, B. Distribution and accumulation of dietary ergothioneine and its metabolites in mouse tissues. *Sci. Rep.* **2018**, *8*, 1–15. [CrossRef]

63. Benoff, S. Receptors and channels regulating acrosome reactions. *Hum. Fertil. (Camb.)* **1999**, *2*, 42–55. [CrossRef]

64. Darszon, A.; Labarca, P.; Nishigaki, T.; Espinosa, F. Ion channels in sperm physiology. *Physiol. Rev.* **1999**, *79*, 481–510. [CrossRef]

65. Benoff, S.; Hurley, I.; Cooper, G.W.; Mandel, F.S.; Rosenfeld, D.L.; Hershlag, A. Head-specific mannose-ligand receptor expression in human spermatozoa is dependent on capacitation-associated membrane cholesterol loss. *Hum. Reprod.* **1993**, *8*, 2141–2154. [CrossRef] [PubMed]

66. Benoff, S.; Cooper, G.W.; Centola, G.M.; Jacob, A.; Hershlag, A.; Hurley, I.R. Metal ions and human sperm mannose receptors. *Andrologia* **2000**, *32*, 317–329. [CrossRef] [PubMed]

67. Wang, R.; Song, B.; Wu, J.; Zhang, Y.; Chen, A.; Shao, L. Potential adverse effects of nanoparticles on the reproductive system. *Int. J. Nanomed.* **2018**, *13*, 8487–8506. [CrossRef]

68. Lansman, J.B. Blockade of current through single calcium channels by trivalent lanthanide cations. Effect of ionic radius on the rates of ion entry and exit. *J. Gen. Physiol.* **1990**, *95*, 679–696. [CrossRef]

69. Thill, A.; Zeyons, O.; Spalla, O.; Chauvat, F.; Rose, J.; Auffan, M.; Flank, A.M. Cytotoxicity of CeO_2 Nanoparticles for Escherichia coli. Physico-Chemical Insight of the Cytotoxicity Mechanism. *Environ. Sci. Technol.* **2006**, *40*, 6151–6156. [CrossRef] [PubMed]

70. Zeyons, O.; Thill, A.; Chauvat, F.; Menguy, N.; Cassier-Chauvat, C.; Oréar, C.; Daraspe, J.; Auffan, M.; Rose, J.; Spalla, O. Direct and indirect CeO_2 nanoparticles toxicity for *Escherichia coli* and *Synechocystis*. *Nanotoxicology* **2009**, *3*, 284–295. [CrossRef]

71. Plakhova, T.V.; Romanchuk, A.Y.; Yakunin, S.N.; Dumas, T.; Demir, S.; Wang, S.; Minasian, S.G.; Shuh, D.K.; Tyliszczak, T.; Shiryaev, A.A.; et al. Solubility of Nanocrystalline Cerium Dioxide: Experimental Data and Thermodynamic Modeling. *J. Phys. Chem. C* **2016**, *120*, 22615–22626. [CrossRef]

72. Lishko, P.V.; Botchkina, I.L.; Fedorenko, A.; Kirichok, Y. Acid extrusion from human spermatozoa is mediated by flagellar voltage-gated proton channel. *Cell* **2010**, *140*, 327–337. [CrossRef] [PubMed]

73. Mehrabi, K.; Nowack, B.; Arroyo Rojas Dasilva, Y.; Mitrano, D.M. Improvements in Nanoparticle Tracking Analysis To Measure Particle Aggregation and Mass Distribution: A Case Study on Engineered Nanomaterial Stability in Incineration Landfill Leachates. *Environ. Sci. Technol.* **2017**, *51*, 5611–5621. [CrossRef]

74. Xia, T.; Kovochich, M.; Brant, J.; Hotze, M.; Sempf, J.; Oberley, T.; Sioutas, C.; Yeh, J.I.; Wiesner, M.R.; Nel, A.E. Comparison of the abilities of ambient and manufactured nanoparticles to induce cellular toxicity according to an oxidative stress paradigm. *Nano Lett.* **2006**, *6*, 1794–1807. [CrossRef]

75. Singh, N.; Manshian, B.; Jenkins, G.J.S.; Griffiths, S.M.; Williams, P.M.; Maffeis, T.G.G.; Wright, C.J.; Doak, S.H. NanoGenotoxicology: The DNA damaging potential of engineered nanomaterials. *Biomaterials* **2009**, *30*, 3891–3914. [CrossRef] [PubMed]

76. Ema, M.; Kobayashi, N.; Naya, M.; Hanai, S.; Nakanishi, J. Reproductive and developmental toxicity studies of manufactured nanomaterials. *Reprod. Toxicol.* **2010**, *30*, 343–352. [CrossRef] [PubMed]

77. Blum, J.L.; Xiong, J.Q.; Hoffman, C.; Zelikoff, J.T. Cadmium Associated With Inhaled Cadmium Oxide Nanoparticles Impacts Fetal and Neonatal Development and Growth. *Toxicol. Sci.* **2012**, *126*, 478–486. [CrossRef] [PubMed]

78. Gao, G.; Ze, Y.; Li, B.; Zhao, X.; Zhang, T.; Sheng, L.; Hu, R.; Gui, S.; Sang, X.; Sun, Q.; et al. Ovarian dysfunction and gene-expressed characteristics of female mice caused by long-term exposure to titanium dioxide nanoparticles. *J. Hazard. Mater.* **2012**, *243*, 19–27. [CrossRef]

79. Tassinari, R.; Cubadda, F.; Moracci, G.; Aureli, F.; D'Amato, M.; Valeri, M.; De Berardis, B.; Raggi, A.; Mantovani, A.; Passeri, D.; et al. Oral, short-term exposure to titanium dioxide nanoparticles in Sprague-Dawley rat: Focus on reproductive and endocrine systems and spleen. *Nanotoxicology* **2014**, *8*, 654–662. [CrossRef]

80. Pietroiusti, A.; Massimiani, M.; Fenoglio, I.; Colonna, M.; Valentini, F.; Palleschi, G.; Camaioni, A.; Magrini, A.; Siracusa, G.; Bergamaschi, A.; et al. Low doses of pristine and oxidized single-wall carbon nanotubes affect mammalian embryonic development. *ACS Nano* **2011**, *5*, 4624–4633. [CrossRef]

81. Williams, R.; Sparacino, C.; Petersen, B.; Bumgarner, J.; Jungers, R.H.; Lewtas, J. Comparative characterization of organic emissions from diesel particles, coke oven mains, roofing tar vapors and cigarette smoke condensate. *Int. J. Environ. Anal. Chem.* **1986**, *26*, 27–49. [CrossRef]

82. Scheepers, P.T.J.; Bos, R.P. Combustion of diesel fuel from a toxicological perspective. *Int. Arch. Occup. Environ. Heath* **1992**, *64*, 149–161. [CrossRef]

83. Brevik, A.; Lindeman, B.; Rusnakova, V.; Olsen, A.-K.; Brunborg, G.; Duale, N. Paternal Benzo[a]pyrene Exposure Affects Gene Expression in the Early Developing Mouse Embryo. *Toxicol. Sci.* **2012**, *129*, 157–165. [CrossRef]